© Universiti Tun Hussein Onn Malaysia Publisher's Office

IJIE

http://penerbit.uthm.edu.my/ojs/index.php/ijie
ISSN : 2229-838X e-ISSN : 2600-7916

The International Journal of Integrated Engineering

Experimental Study and Exergy Analysis About the Flat Plate Solar Collector

Fadhil Abdulrazzaq Kareem [1], Osamah Raad Skheal [2*], Noor Samir Lafta [3]

[1]Middle Technical University, Baghdad, Iraq – Institute of Technology, Baghdad, 10074, IRAQ

[2]Middle Technical University, Baghdad, Iraq – Technical Instructors Training Institute, Hilla, 51001, IRAQ

[3]Middle Technical University, Baghdad, Iraq – Institute of Technology, Baghdad, 10076, IRAQ

*Corresponding Author

DOI: https://doi.org/10.30880/ijie.2022.14.06.014
Received 15 October 2021; Accepted 11 October 2022; Available online 10 November 2022

Abstract: The increase of clean energy requirement is still enhanced in order to reduce the effect of the global warming therefore, the augmentation of solar energy applications like the solar collectors is attended. The present study of the Flat Plate Solar Collector (FPSC) is performed during the three days' time (2,3 and 4 of June). Where, the testing time is specified from 09:00Am up to 03:00Pm in order to give more obvious data. Moreover, the energy and exergy analysis equations are utilized to study the 1st and 2nd law of thermodynamics and to provide more appropriate results about the performance of the FPSC. The conducted results show an enhancement in the FPSC efficiency with respect to the increase of the solar irradiance where the last one was explained through one-day time. Furthermore, the FBSC exergy and energy efficiencies conduct the same behaviors during the daytime due to the effect of the solar radiation. In addition, the useful exergy and the exergy efficiency are raised with the progression of time until it reaches approximately midday and then dropped down because of the solar radiation reduction.

Keywords: Exergy analysis, solar collector, exergy efficiency, useful exergy, exergy destruction.

1. Introduction

Solar energy is the cleanest and future energy that is promised to be used in the next time. Solar energy can be useful when it extracted as heat energy or electrical one therefore, it so important to develop the denoted applications to give us best income. One of the famous applications in the solar energy are the solar collectors in which used to collect the solar radiation and convert it into pure heat energy. This application is so useful to provide the hot water by clean heat energy without fuel burning or electrical consumption [1].

The use of the thermosiphon to the flat plat solar collector tended to increase the performance of it clearly. Also, it was achieved that there were no effects to utilize the aluminum plate or cupper plate as the absorber over the collector. Therefore, Aluminum was proposed to be used throughout the present work [2]. Furthermore, the entire tubes in which were carrying the working fluid geometry played an important rule to enhance the exergy efficiency when the elliptical shapes were selected. Moreover, the Nano-fluid with turbulent behavior gave a good enhancement in the overall thermal performance of the solar collector [3], [4]. By the addition, The Nano-fluid utilization as working fluid revealed that the overall thermal efficiency was increased noticeably [5]. The previous studies led us to study the collector with circular shape section without any addition to the Nano-particles due to the hazard of use them on the human health [6].

*Corresponding author: osamaraad19@yahoo.com

The increase of the mass flow rate of the working fluid inside the solar collector tubes tended to enhance the first and second law of the thermodynamic efficiencies [7]. Thus, the fabrication of the used rig of the present study was depended on the previous. The most efficient solar collector was achieved when the absorber temperature become more closed to the ambient one. Furthermore, the rise of the working fluid flowrate tended to decline the absorber temperature. This one acted on specifying the range of flowrate within the active limits [8]. The higher insulation layer at the back of the flat solar collector conducted a soar in the second law efficiency. It was also, noticed that high inlet fluid temperature to the collector and high wind speed plummeted the exergy efficiency [9]. The productive amount of the hot water was growing with the increase of the daily solar active hours respectively. Furthermore, it was noticed that the first law efficiency was increased by the same previous manner [10], [11]. The higher mass flow rate of the collector working fluid went up the energy efficiency up to certain value then it will be stabilized in spite of adding more flowrate. Furthermore, the exergy efficiency tended to soar under limited value of flowrate then it declined by the increase of the flowrate [12]. The second law efficiency depended on the solar radiation, ambient temperature, wind velocity, water inlet and outlet temperature, and environmental situation [13]. The second law efficiency was referred to be enhanced by enhancing the thermal insulation of the flat plate solar collector. Moreover, it was declined by increasing the ambient temperature [14]. The optical efficiency of the absorber conducted a clear effect on the exergy efficiency by knowing that the emittance and absorbance were the prime mover of the optical efficiency [1]. The outlet productive heat energy was raised by the increase of the solar irradiance and the ambient temperature [15]. The use of the textile fabric as absorber for the solar collector presented high qualification in the thermal performance as compared to the common flat plat one [16]. The activity of the solar radiation changes according to the location and the weather. Therefore, it was considered that the solar collector performance gave a limited heat energy which corresponded the solar irradiance [17]. Moreover, the presence of air inside the collectors declined its energy and exergy efficiencies as compared to the evacuated ones due to the air heat capacity [18].

According to the previous it was tended to investigate the energy and exergy analysis on the flat plate solar collector in order to form a wide area knowledge about it during one day and multiday. Furthermore, the first and the second laws of thermodynamic analysis are aimed to be discussed there.

2. Experimental Methodology

The experimental was conducted in Iraq, Baghdad (33.3 N latitude, 44.2 E longitude). The FPC is manufactured and built by the authors, it consists of glass cover, absorb plate, frame, insulation, rise and header pipe, water tank, pump, valve and measurement devices. The collector frame is insulated at bottom and side, while the surface is covered by single glass. The FPC consists of two headers and ten rise pipes. A schematic diagram of the apparatus is shown in Fig. 1. The specification of experimental setup is shown in Table 1. The analysis has been developed by using (EES) software. The environmental parameter of solar radiation, ambient temperature, and wind speed are obtained using Metronome software. The experimental test collected every hour interval during 9:00 to 15:00 of a full day time, the cold water feed the FPC and it absorbs solar energy that fall in the glass of the collector as a results the temperature of cold water increase. The hot water from FPC flow to the tank by force circulates (pump), and the storage tank exchange heat with secondary fluid. The flow rate of the cold water entering to FPC is controlled by manual valve. The temperature of inlet and outlet water from FPC was measure by using K type thermocouple with a precision of ± 0.45 C, and the flow rate of water that supply to the FPC was measure by using water flow-meter with a precision of ± 0.25 L/min.

Table 1 - Specification of FPC

Collector details	Specification
Type	Flat plate solar collector
Absorb area	1.5 m2
Absorber plate material	Aluminum
Thermal conductivity of aluminum absorber plate	237 W/(mK)
Absorber Plate thickness	0.25 mm
Space between glass and absorber plate	30 mm
Tilt angle	40 O
Transparent cover	glass
Number of Transparent cover	single
Thickness of Transparent cover	3 mm
thermal insulation	glass wool
Thickness thermal insulation	50 mm

Thermal conductivity thermal insulation	0.034 W/m2K

3. Energy and Exergy Analysis

The first law of thermodynamics is commonly used for analysis and design of thermal system, it is related to conservation of energy and does not provide information about energy losses and irreversibility. So that the second law of thermodynamics is a suitable method to design and analysis of thermal system. It is used to estimate where the irreversibility occurs, exergy destruction, exergy efficiency. The mass conservation, energy conservation, entropy conservation and availability balance can be written as follows [19]

The mass conservation:

$$\frac{dm_{CV}}{dt} = \sum \dot{m}_i - \sum \dot{m}_e \quad (1)$$

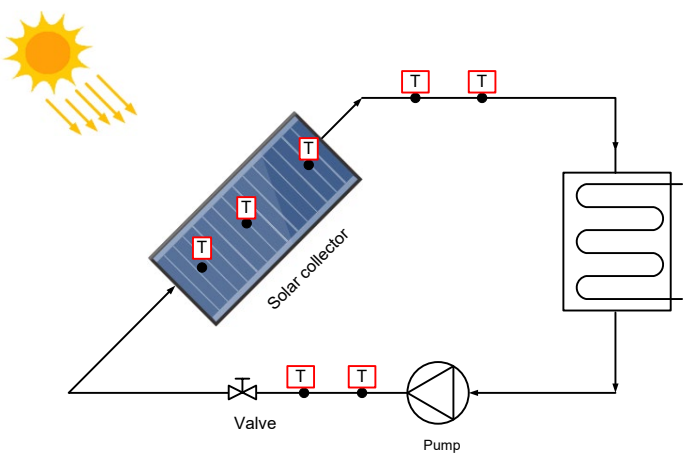

Schematic diagram of flat plate collector

Photograph *of* experimental *test* rig

Fig. 1 - Test rig

Where

$\frac{dm_{CV}}{dt}$ is the rate of mass change in control volume (CV)

$\sum \dot{m}_i$ total mass inlet to CV

$\sum \dot{m}_e$ total mass outlet from CV

The energy conservation:

$$\frac{dE_{CV}}{dt} = \dot{Q}_{CV} - \dot{W}_{CV} + \sum \dot{m}_i \left(h_i + \frac{v_i^2}{2} + gz_i\right) - \sum \dot{m}_e \left(h_e + \frac{v_e^2}{2} + gz_e\right) \quad (2)$$

Where

$\frac{dE_{CV}}{dt}$ is the rate of energy change in control volume (CV)

$\dot{Q}_{CV}$ total heat (in/out) for CV

$\dot{W}_{CV}$ total work (in/out) for CV

h_i, h_e enthalpy of the fluid inlet and outlet from CV respectively

v_i, v_e velocity (kinetic energy) of the fluid inlet and outlet from CV respectively

z_i, z_e elevation (potential energy) of the fluid inlet and outlet from CV respectively

The entropy balance

$$\frac{dS_{CV}}{dt} = \sum \dot{m}_i s_i - \sum \dot{m}_e s_e + \sum \frac{\dot{Q}_{CV}}{T} + \dot{S}_g \quad (3)$$

Where
$\frac{dS_{CV}}{dt}$ is the rate of entropy change in control volume (CV)
s_i, s_e enthalpy of the fluid inlet and outlet from CV respectively
$\dot{S}_g$ rate of entropy generation within CV
T the temperature of heat source

The exergy balance

$$\frac{d\Phi_{CV}}{dt} = \sum \dot{Q}_{CV}\left(1 - \frac{T_o}{T}\right) - \dot{W}_{CV} + P_o \frac{dV}{dt} + \sum \dot{m}_i \psi_i - \sum \dot{m}_e \psi_e - T_o \dot{S}_g \quad (4)$$

Where
$\frac{d\Phi_{CV}}{dt}$ is the rate of exergy change in control volume (CV)
T_o the reference temperature
$P_o \frac{dV}{dt}$ is the boundary work
ψ_i, ψ_e exergy transfer by flow, which can be estimated as [19]:

$$\psi = (h - h_o) - T_o(s - s_o) \quad (5)$$

The following assumptions are suggested to simplify the models:
(1) The FPC is a steady-state condition.
(2) Uniform flow rate inside tubes.
(3) Neglected pressure drop of the fluid inside tubes.
(4) Neglected pump work.

3.1 Energy Analysis

Based on the ASHRAE standard 2011 [20] the amount of heat energy ($\dot{Q}_{in}$) that received by the collector is:

$$\dot{Q}_{in} = G * A * (\tau\alpha)_\theta \quad (6)$$

Where
G: solar incident radiation falls on the earth (W/m2)
A: area of collector
$(\tau\alpha)_\theta$: Transmittance τ of cover times absorptance α of plate at prevailing incident angle θ [20]

The rate of heat loss ($\dot{Q}_{out}$) depends on the overall heat transfer coefficient (U_L) of the FPC,the collector temperature (T_c) and the ambient temperature (T_a) [21]

$$\dot{Q}_{out} = U_L * A * (T_c - T_a) \quad (7)$$

Thus, the rate of useful energy of the FPC ($\dot{Q}_{useful}$) is proportional to the rate of energy absorbed by the collector ($\dot{Q}_{in}$), minus the energy lost by the collector ($\dot{Q}_{out}$)

$$\dot{Q}_{useful} = \dot{Q}_{in} - \dot{Q}_{out} \quad (8)$$

It is also that can be known that the amount of heat carried away in the fluid passed through it

$$\dot{Q}_{useful} = \dot{m} * Cp * \left(T_{f,o} - T_{f,i}\right) \tag{9}$$

Where $\dot{m}$ is mass flow rate of fluid (kg/s), Cp specific heat of fluid (kJ/kgK), $T_{f,o}$ outlet fluid temperature from FPC, and $T_{f,i}$ inlet fluid temperature to FPC.

The energy efficiency is defined as the ratio of useful energy of the FPC to the heat energy received by FPC. The energy efficiency of the FPC is [21]:

$$\eta = \frac{Q_{useful}}{G*A} \tag{10}$$

It is also that can be calculated by using ASHRAE standard 2011 [20] correlation:

$$\eta = F_R\left[(\tau\alpha)_\theta - U_L\frac{(T_{f,i}-T_a)}{G}\right] \tag{11}$$

Where F_R is the collector heat removal factor

3.2 Exergy Analysis

In order to obtain a better design and analysis it is important to link the first and second law of thermodynamics where, the exergy is the term that deal with these two laws. It can be defining as a maximum work that can be product from system when the system become at dead state.

The inlet exergy rate that carried by the working fluid with assuming the exergy loss due to the fluid pressure drop inside collector tubes to be negligible, the inlet exergy rate is given as follows [22]

$$Ex_{f,i} = \dot{m} * cp * \left(T_{f,i} - T_a - T_a \ln\left(\frac{T_{f,i}}{T_a}\right)\right) \tag{12}$$

The outlet exergy rate is given by [22]

$$Ex_{f,o} = \dot{m} * cp * \left(T_{f,o} - T_a - T_a \ln\left(\frac{T_{f,o}}{T_a}\right)\right) \tag{13}$$

The useful exergy rate that can be obtain from FPC is estimated by

$$Ex_{useful} = Ex_{f,o} - Ex_{f,i} \tag{14}$$

The rate of exergy losses in the FPC is divided into four parts [23]. The first part is the rate of exergy losses between absorber plate and the sun due to temperature differences [22,23]

$$Ex_{p,s} = G * A * (\tau\alpha)_\theta * T_a * \left(\frac{1}{T_p} - \frac{1}{T_s}\right) \tag{15}$$

Where T_p is plate temperature and can be calculated by [24]

$$T_p = T_{f,i} + \frac{Q_{useful}}{A*U_L*F_R}(1 - F_R) \tag{16}$$

And T_s is the sun temperature and it is equal to 6000 K [25,26]

The second part is the rate of exergy losses from FPC surface to the absorber plate [23]

$$Ex_{c,p} = G * \left(A - (\tau\alpha)_\theta * A_p\right)\left(1 - \frac{T_a}{T_s}\right) \tag{17}$$

The third part is the rate of exergy losses between absorber plate and fluid due to temperature differences [22, 23]

$$Ex_{p,f} = \dot{m} * cp * T_a * \left(\ln\left(\frac{T_{f,o}}{T_{f,i}}\right) - \frac{T_{f,o}-T_{f,i}}{T_p}\right) \quad (18)$$

The fourth part is the rate of exergy losses from absorber plate to environmental [22,23]

$$Ex_{p,e} = U_L * A * \left(T_p - T_a\right)\left(1 - \frac{T_a}{T_p}\right) \quad (19)$$

The exergy destruction rate of the FPC can be defined as [27]

$$Ex_{dest.} = \dot{S}_{gen.} * T_a \quad (20)$$

The overall entropy generation of the FPC can calculated [27]

$$\dot{S}_{gen.} = \dot{m} * cp * \ln\left(\frac{T_{f,o}}{T_{f,i}}\right) - \frac{\dot{Q}_{in}}{T_s} + \frac{\dot{Q}_{loss}}{T_a} \quad (21)$$

Where $\dot{Q}_{loss}$ is the rate of heat lost to the environment, which can be calculated by [27]

$$\dot{Q}_{loss} = \dot{Q}_{in} - \dot{Q}_{useful} \quad (22)$$

The exergy efficiency can be calculated as follows [22,23,27]

$$\eta_{ex} = \frac{Ex_{useful}}{Ex_{sol.}} \quad (23)$$

Where $Ex_{sol.}$ Is the solar radiation exergy, which can be calculated by [24]

$$Ex_{sol.} = G * A * \left(1 - \frac{4}{3}\left(\frac{T_a}{T_s}\right) + \frac{1}{3}\left(\frac{T_a}{T_s}\right)^4\right) \quad (24)$$

The uncertainty analysis is important to improve the accuracy of the used measurement devices. Thus, uncertainties can be estimation by:

$$U_R = \left[\left(\frac{\partial R}{\partial x_1} U_1\right)^2 + \left(\frac{\partial R}{\partial x_2} U_2\right)^2 + \cdots + \left(\frac{\partial R}{\partial x_n} U_n\right)^2\right]^{\frac{1}{2}} \quad (25)$$

where U_R denotes total uncertainty, R is a given function, x1, x2, …,xn are independent variables, U_1, U_2, …, U_n are uncertainty in the independent variables. The summarized analysis of the experimental accuracy of the measuring properties of some selected measuring devices is shown in Table 2

Finally, the uncertainties for the estimation parameters such energy efficiency and exergy efficiency and exergy are 1.53%, 0.87% and 0.95%, respectively.

Table 2 - Experimental accuracy

Independent variables	Uncertainty interval
K type thermocouple	± 0.45 C
Temperature readers	± 1 ºC
water flow-meter	± 0.25 L/min.

4. Result and Discussion

In this research, a lot of energy and exergy analysis have been calculated and analyzed to know the losses that occur when converting solar energy by using the flat plate solar collector. A set of losses and their relationships with time are performed. Also, it is tended to use another variable like the flowrate with different values such as (0.01, 0.015, 0.02) Kg/sec respectively.

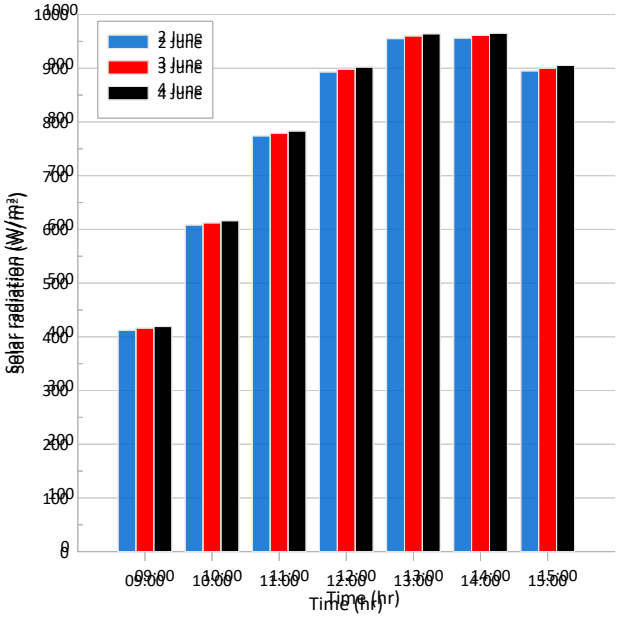

Fig. 2 - Solar radiation for three days in June

Fig. (2) shows that the solar irradiation for three days (2, 3, 4) through June month day time of 9:00 am to 3:00 pm. It also shows that the highest radiation has been notified at 2:00 pm for these three days while the highest value during the June season is 965 w/m2. A little increase is achieved for the solar radiation during the denoted three tested days gradually where this one is done due to the increase of the active radiation angle of the sun for the testing zone. Moreover, the activity of the solar day time is conducted very well because of the increase of the solar radiation up to the mid-day time and then goes down after that time.

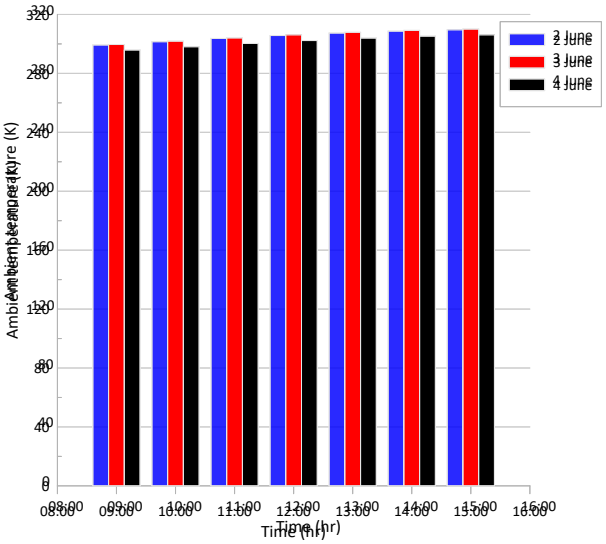

Fig. 3 - Ambient temperature for three days in June

Fig. (3) represents the relationship between the ambient temperatures with time. It is noticed that the increase in the ambient temperature begins gradually from 9:00 am to 3:00 pm consciously at 3:00 pm while the highest values are observed at 3:00 pm with an ambient temperature of 37.1 ºC. The ambient temperature is the most important factor that

effect on the exergy destruction, exergy useful and exergy efficiency of the collector. As a result of increase in difference between ambient temperature and collector temperature exergy destruction is rise while, exergy efficiency is drop. Fig. (4) shows the relationship between the plate temperature and the time for the days (2, 3, and 4)of June within 9:00 am to 3:00 pm, where the plate temperature begins to rise as time progresses as a result of the increase in the external temperature until it reaches a peak at 2 pm. the plate temperature play a significant factor that effect on the collector performance the temperature of its was depended on the overall heat transfer coefficient of the collector (insulation) ant the materials type of the plate. Fig. (5) above explains the increase of the heat transfer rate of the flat plate solar collector (FPSC) for the daytime duration. This one is satisfying the increase of the solar irradiance due to the sun titled angle from the sun raise up to the middle day. Furthermore, the enhancement in the heat transfer rate by the increase of the mass flow rate during the day time is observed with best values as 924W and 0.02 kg/s respectively. Where, the last one is conducted and satisfied according to the governing equation Eq.8.

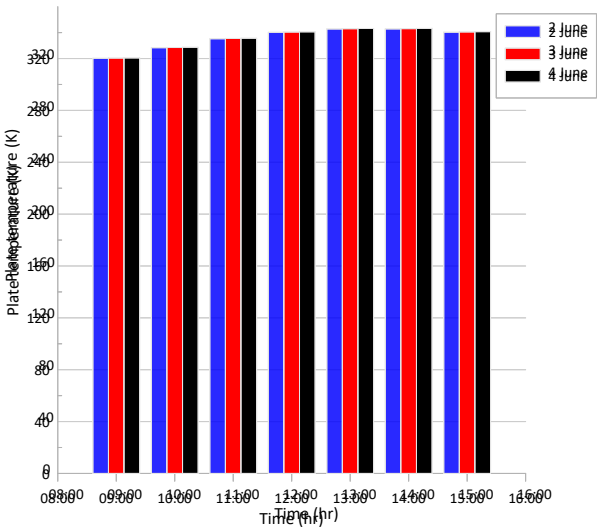

Fig. 4 - Change of plate temperature with time for three days in June

Fig. (6) provides a good representation of the energy efficiency of the used solar collector throughout the daytime. It is noticed that the efficiency of it tended to increase by the increase of the solar irradiance intensity up to the middle of the day. The increase of the efficiencies values is due to the increase in the affected temperatures of the used working fluid and the temperature of the solar collector absorber. The specified day time is selected from 09:00 am up to 03:00 pm. Three values of the working fluid flow rates are examined experimentally and theoretically where the Fig.6 above shows the comparison among them. Moreover, it shows that there is a convergence between the experimental and theoretical results. It is also explained some abnormal values in which can be noticed within the experimental result line. These divergent results may be executed due to different factors such as measurement devices uncertainties, operation conditions, and environmental conditions. The energy efficiency enhancement as compared to the time propagation is observed with best values of 0.02 kg\s, 73%, and 68.06% as mass flow rate, theoretical and experimental efficiencies respectively. The percentage error between theoretical and experimental results are (11%, 10.6%, 13.8%) with respect to the three flow rates values (0.01, 0.015, 0.02) kg\sec respectively. It is noticed that a clear deviation between the experimental and theoretical results where this is due to the effect of the heat transfer losses to the ambient, thermal conductivity of the aluminum plate and the uncertainty of the used measurement devices. Thus, the experimental results do not reach the ideality of the theoretical ones.

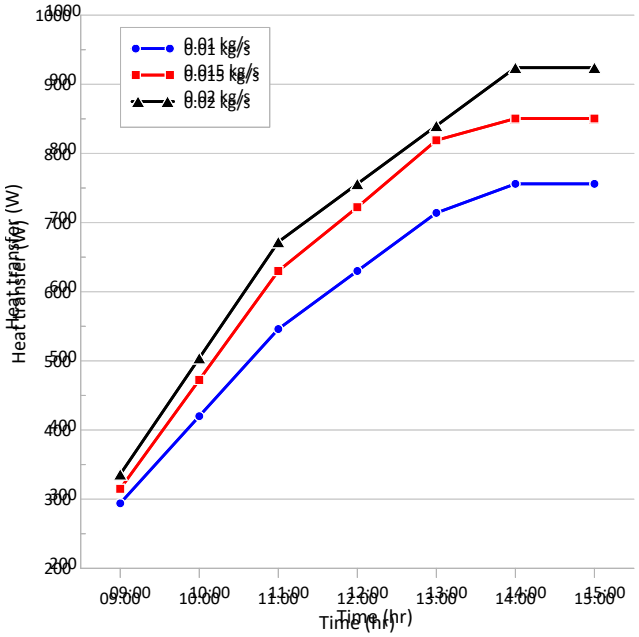

Fig. 5 - Change of heat transfer with time by variation of mass flow rate

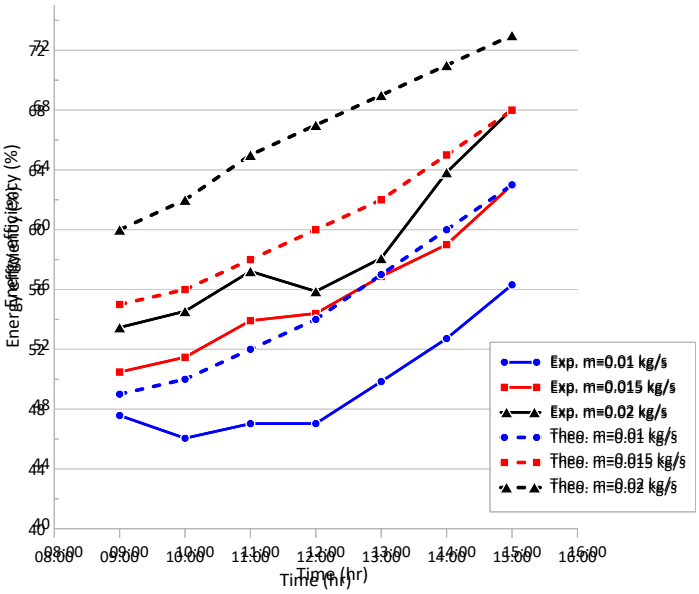

Fig. 6 - Change of energy efficiency with time and comparison between theoretical and experimental

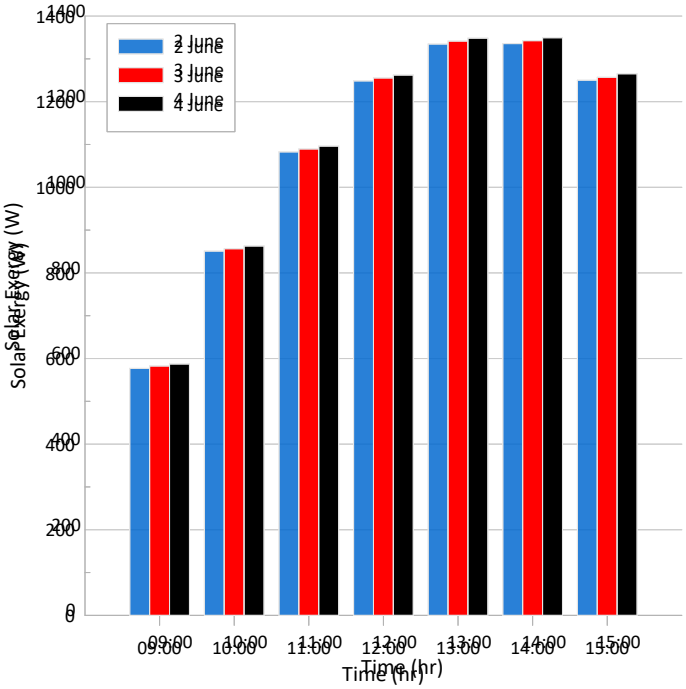

Fig. 7 - Change of solar exergy for three days in June

The second law analysis becomes a good comparison factor to get on the thermal performance of any thermal application. Therefore, Fig. (7) shows the soar of the FPSC exergy efficiency during the operation day time (09:00 am – 03:00 pm). It is well known that all the incident solar radiation is not usable energy. Since there is no simultaneous absorption of solar radiation due to reflection, absorption, and heat losses with ambient. Thus, it is clear that solar incident is more than solar exergy. As well as, this Fig. shows that the highest solar exergy is on the 4th of June at the hour 2 pm.

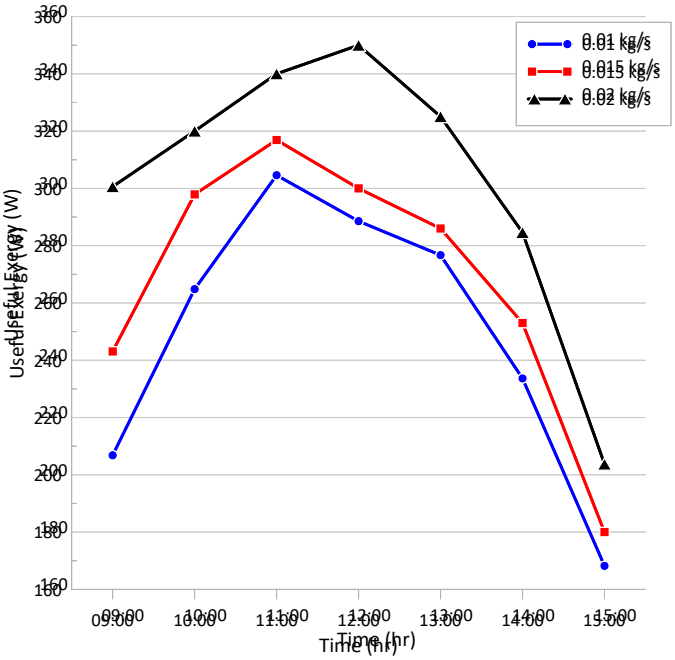

Fig. 8 - Change of useful exergy with time by variation mass flowrate

The useful exergy of the flat plate solar collector (FPSC) for the daytime duration was presented in Fig. (8). It can be noticed that the useful exergy starts by the daytime increasing up to 11:00 am and 12:00 pm and then decreases with the progression of time, according to the amount of flow, and the reason for this is that the useful exergy is affected by several factors, including solar radiation, ambient temperature, dust in the air and wind, as the radiation gradually

begins to increase with the progression of time. the useful exergy begins to decrease at 11 am due to the ambient temperature play a significant factor in the exergy performance of FPSC more than solar radiation and another factor, reaching 305 watts. When the flow is 0.01 kg/s at 11 am, which is the highest value at this flow, and it is 318 watts when the flow is 0.015 kg/s, which is the highest value for this flow, and it reaches 348 watts when the rate of flow is 0.02 kg/s and then the useful losses begin to decrease, as we note through these values that the useful losses increase with increase The flow, because it is directly proportional to the increase in the rate of flow, and this is shown by its equation.

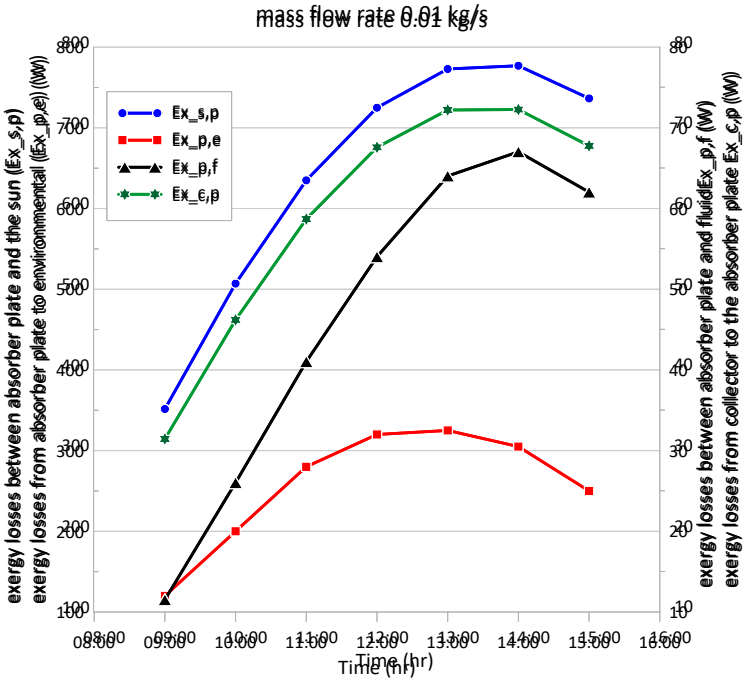

Fig. 9 (a) - Change in the rate of exergy losses between absorber plate and the sun (Ex_s, p), the rate of exergy losses from absorber plate to environmental (Ex_ p,e), the rate of exergy losses between absorber plate and fluid (Ex_p,f), the rate of exergy losses from collector to the absorber plate (Ex_c,p) with time for 0.01 kg/s

The variation rate of exergy losses between absorber plate and the sun (Ex_s, p), rate of exergy losses from FPC surface to the absorber plate (Ex_c,p), rate of exergy losses between absorber plate and fluid (Ex_p,f), and rate of exergy losses from absorber plate to environmental (Ex_ p,e) concerning the day time duration was presented in Fig. (9-A, B, C). Fig. A at the flow rate is 0.01kg/s and Fig. B has the flow rate of 0.015 kg/s and in Fig. C the flow rate is 0.02 kg/s. Through these Fig.s, we note that the highest values of EX_s,p, EX_p,e, EX_c, p, and Ex_p,f were (784 W, 400.4 W, 74.3 W, 49.8 W), respectively, at 1:30 pm and a flow rate of 0.02 kg/sec. each part of the loss is affected by a different factor, the exergy loss rate caused by the temperature difference between the absorber plate surface and the sun (Ex_s, p) depended on the average absorber plate temperature and radiative heat transfer. The exergy loss rate caused by the temperature difference between a surface collector and plate (Ex_c,p) depended strongly on the physical properties of the materials that construction them. The exergy loss rate caused by the temperature difference between the absorber plate and fluid (Ex_p,f) depended on fluid temperature and plate temperature as an increase in the difference of the absorber plate lead to an increase in this part of the exergy loss rate. Finally, the insulation and temperature differences play a significant factor that affects the exergy loss rate caused by the temperature difference between plate and environmental (Ex_ p,e).

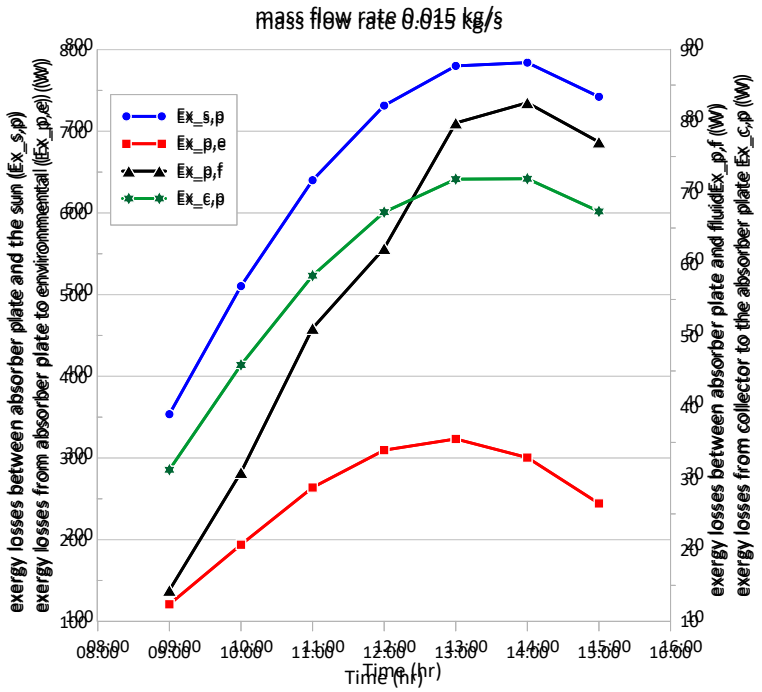

Fig. 9 (b) - Change in the rate of exergy losses between absorber plate and the sun (Ex_s, p), the rate of exergy losses from absorber plate to environmental (Ex_ p,e), the rate of exergy losses between absorber plate and fluid (Ex_p,f), the rate of exergy losses from collector to the absorber plate (Ex_c,p) with time for 0.015 kg/s

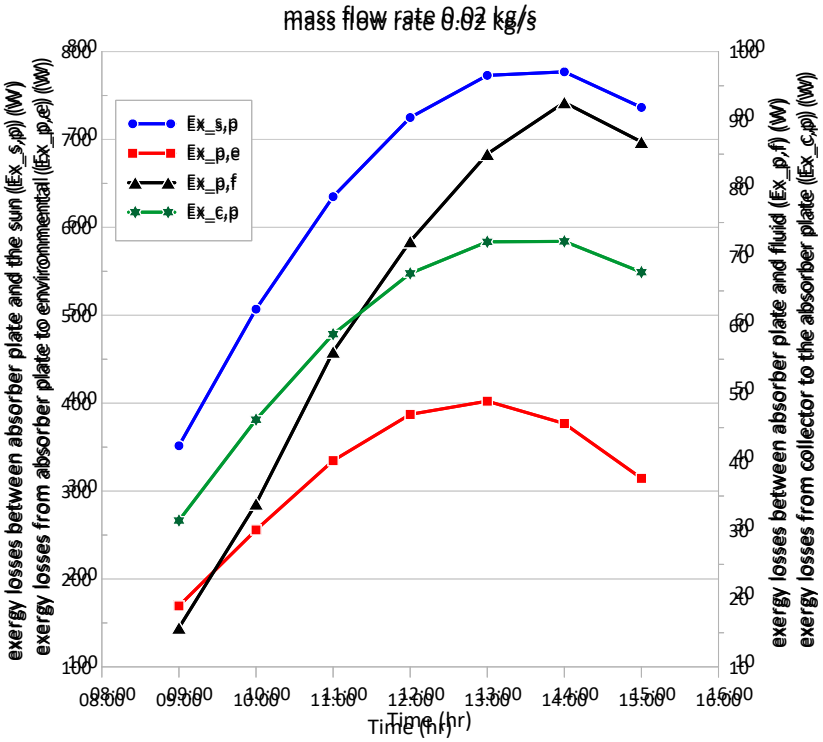

Fig.9 (c) – Change in the rate of exergy losses between absorber plate and the sun (Ex_s, p), the rate of exergy losses from absorber plate to environmental (Ex_ p,e), the rate of exergy losses between absorber plate and fluid (Ex_p,f), the rate of exergy losses from collector to the absorber plate (Ex_c,p) with time for 0.02 kg/s

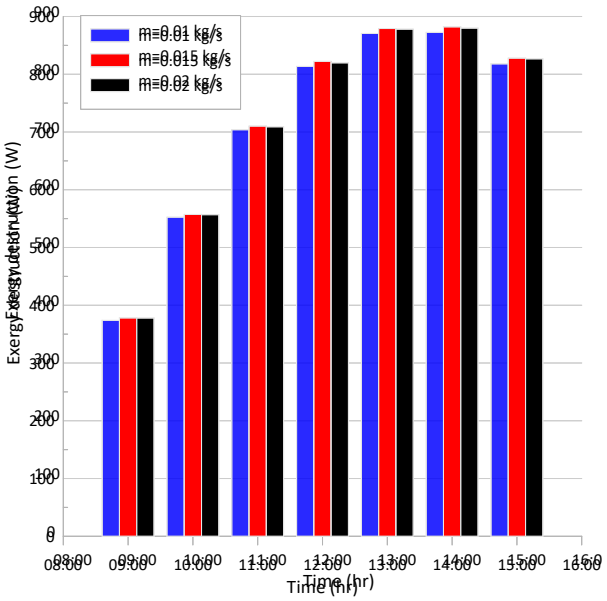

Fig. 10 - Change the exergy destruction with time by variation mass flow rate

Fig. (10) illustrates the relationship between the exergy destruction with time and the change in the rate of flow, as work was carried out during the period from 9 am to 3 pm and with a change of flowrate (0.01, 0.015, 0.02) kg/s, where we note that the exergy destruction increases with the progression of time as a result of the increase in the ambient temperature and the amount of radiation because it is a direct proportion between them. We also note that it increases with an increase in the flow rate to reach the highest value when the flow rate is 0.02 kg / s at 2 pm, and this is illustrated by the following values (872.4, 882.1, 879.9) Watts for flow rates (0.01, 0.015, 0.02) kg/s respectively

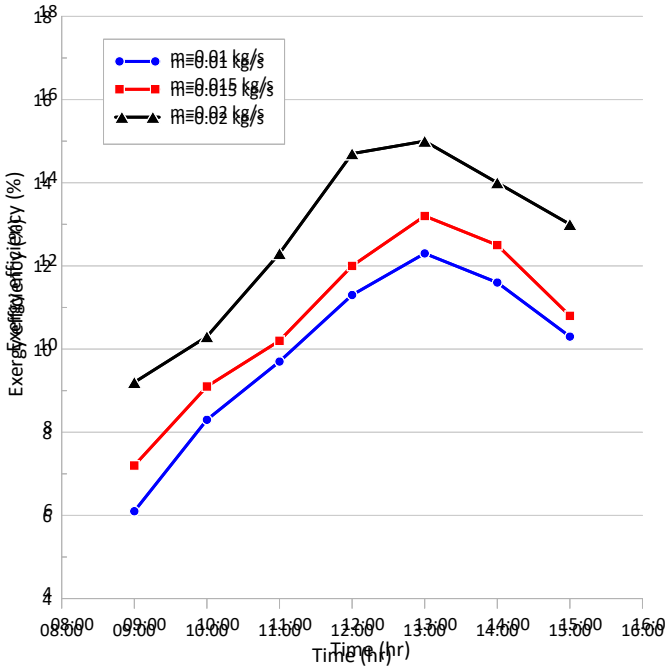

Fig. 11 - Change of exergy efficiency with time by variation of mass flow rate

Fig. 11 shows the relationship between the exergy efficiency with time, as work was carried out during the period from 9 am to 3 pm and with the change of three flow values (0.01, 0.015, 0.02) kg / s. The weather data included global solar radiation on an inclined surface, ambient temperature, and wind speed, which are considered when calculating the FPSC exergy. where we note that the exergy efficiency increases with the progression of time as a result of the increase in the degree of Heat and the amount of radiation because it is a direct proportion between them, and this is explained by the equation for the efficiency of losses, and we also notice that it increases by increasing the flow rate to reach the highest value when the flow rate is 0.02 kg/sec at 2 pm.

5. Conclusion

From the weather data and applied the second law of thermodynamic on the FPSC system, it can be concluded that:

1- Due to the increase in temperature difference, heat transfer between solar radiation and fluid increases with time, resulting in an increase in energy efficiency, with the best values of heat transfer to the collector being 924W for 0.02 kg/s.
2- The solar incident is more than solar exergy because it is affected by several factors, including high temperature, solar radiation, wind speed, and dust in the air.
3- The best values of theoretical and experimental efficiencies at flow 0.02 kg/s were 73 percent, and 68.06 percent respectively.
4- With respect to the three flow rate values (0.01, 0.015, and 0.02) kg/sec, the error obtained between theoretical and experimental results is (11 percent, 10.6 percent, 13.8 percent).
5- The useful exergy increases with the progression of time until it reaches approximately midday and then begins to decrease very quickly because it is affected by environmental factors.
6- At 1:30 pm and a flow rate of 0.02 kg/sec, the maximum values of the change in the rate of exergy losses between absorber plate and the sun (Ex_s, p), the rate of exergy losses from absorber plate to environmental (Ex_ p,e), the rate of exergy losses between absorber plate and fluid (Ex_p,f),and the rate of exergy losses from collector to the absorber plate (Ex_c,p) were (784 W, 400.4 W, 74.3 W, and 49.8 W, respectively.
7- The exergy efficiency for mass flow rate 0.02 kg/s improves with the progression of time until it reaches 2 p.m., when it achieves its peak, and then begins to decrease as the temperature and radiation begin to decrease.

Acknowledgement

The authors would like to thanks the Middle Technical University for giving the opportunity to conduct this research.

References

[1] Shamshirgaran, S. R., Khalaji Assadi, M., Badescu, V. & Al-Kayiem, H. H. Upper limits for the work extraction by nanofluid-filled selective flat-plate solar collectors. *Energy* **160**, 875–885 (2018).
[2] Wenceslas, K. Y. & Ghislain, T. Experimental Validation of Exergy Optimization of a Flat-Plate Solar Collector in a Thermosyphon Solar Water Heater. *Arab. J. Sci. Eng.* **44**, 2535–2549 (2019).
[3] Rostami, S. *et al.* Exergy optimization of a solar collector in flat plate shape equipped with elliptical pipes filled with turbulent nanofluid flow: A study for thermal management. *Water (Switzerland)* **12**, (2020).
[4] Eltaweel, M. & Abdel-Rehim, A. A. Energy and exergy analysis of a thermosiphon and forced-circulation flat-plate solar collector using MWCNT/Water nanofluid. *Case Stud. Therm. Eng.* **14**, 100416 (2019).
[5] Alklaibi, A. M., Sundar, L. S. & Sousa, A. C. M. Experimental analysis of exergy efficiency and entropy generation of diamond/water nanofluids flow in a thermosyphon flat plate solar collector. *Int. Commun. Heat Mass Transf.* **120**, 105057 (2021).
[6] Lee, N., Lim, C. H., Kim, T. & Son, E. K. Who Guidelines On Protecting Workers From Which hazard category should specific nanomaterials or groups of nanomaterials be assigned to and how ? *World Heal. Organ.* (2017).
[7] Pathak, P. K., Chandra, P. & Raj, G. Comparative analysis of modified and convectional dual purpose solar collector: Energy and exergy analysis. *Energy Sources, Part A Recover. Util. Environ. Eff.* **00**, 1–17 (2019).
[8] Sinda, A., Ali, S. & Ben Brahim, A. Thermal analysis and exergetic performance of solar flat plate collectors. *2012 1st Int. Conf. Renew. Energies Veh. Technol. REVET 2012* 440–445 (2012) doi:10.1109/REVET.2012.6195310.
[9] Tong, Y., Lee, H., Kang, W. & Cho, H. Energy and exergy comparison of a flat-plate solar collector using water , Al 2 O 3 nanofluid , and CuO nanofluid. *Appl. Therm. Eng.* 113959 (2019) doi:10.1016/j.applthermaleng.2019.113959.
[10] Deniz, E. Energy and exergy analysis of flat plate solar collector-assisted active solar distillation system. *Desalin. Water Treat.* **57**, 24313–24321 (2016).
[11] Abuşka, M. & Şevik, S. Energy, exergy, economic and environmental (4E) analyses of flat-plate and V-groove solar air collectors based on aluminium and copper. *Sol. Energy* **158**, 259–277 (2017).
[12] Das, S. Simulation of optimal exergy efficiency of solar flat plate collector. *Jordan J. Mech. Ind. Eng.* **10**, 51–65 (2016).
[13] Fudholi, A. & Sopian, K. A review of solar air flat plate collector for drying application. *Renew. Sustain. Energy Rev.* **102**, 333–345 (2019).
[14] Gunjo, D. G., Mahanta, P. & Robi, P. S. Exergy and energy analysis of a novel type solar collector under steady state condition: Experimental and CFD analysis. *Renew. Energy* **114**, 655–669 (2017).

[15] Ge, Z., Wang, H., Wang, H., Zhang, S. & Guan, X. Exergy Analysis of Flat Plate Solar Collectors. 2549–2567 (2014) doi:10.3390/e16052549.
[16] Ural, T. Experimental performance assessment of a new flat-plate solar air collector having textile fabric as absorber using energy and exergy analyses. *Energy* **188**, 116116 (2019).
[17] Ben Khedher, N. Experimental Evaluation of a Flat Plate Solar Collector Under Hail City Climate. *Eng. Technol. Appl. Sci. Res.* **8**, 2750–2754 (2018).
[18] Gao, D. *et al.* Experimental and numerical analysis of an efficiently optimized evacuated flat plate solar collector under medium temperature. *Appl. Energy* **269**, 115129 (2020).
[19] Fundamentals of thermodynamics, seventh edition, by Claus Borgnakke and Richard e. Sonntag, 2006, John Wiley & Sons, Inc. ISBN-13 978-0-470-04192-5, Printed in the United States of America
[20] American society of heating, refrigerating & air conditioning engineers, standard 2011, Methods of testing to determine the thermal performance of solar collectors, ASHRAE, 2011
[21] Nidhal Ben Khedher," Experimental Evaluation of a Flat Plate Solar Collector Under Hail City Climate", Engineering, Technology & Applied Science Research, Vol. 8, No. 2, 2018, 2750-2754
[22] Koholé Yemeli Wenceslas, Tchuen Ghislain, "Experimental Validation of Exergy Optimization of a Flat-Plate Solar Collector in a Thermosyphon Solar Water Heater", Arabian Journal for Science and Engineering (2019) 44:2535–2549
[23] Zhong Ge, Huitao Wang, Hua Wang, Songyuan Zhang and Xin Guan, "Exergy Analysis of Flat Plate Solar Collectors", Entropy 2014, 16, 2549-2567; doi:10.3390/e16052549
[24] Verma SK, Sharma K, Gupta NK, Soni P, Upadhyay N, "Performance comparison of innovative spiral shaped solar collector design with conventional flat plate solar collector", Energy, Volume 194, 1 March 2020, 116853 (2020), doi:https://doi.org/10.1016/j.energy.2019.116853.
[25] Fadhil Abdulrazzaq Kareem, Doaa Zaid Khalaf, Noor Samir Lafta, Yasser Abdul Lateef (2019). Energy and Exergy Analysis of a Solar Photovoltaic Performance In Baghdad. Journal of Mechanical Engineering Research & Developments, 42(2): 44-49.
[26] Fadhil Abdulrazzaq Kareem et al 2019 IOP Conf. Ser.: Mater. Sci. Eng. 518 032008
[27] Mahmoud Eltaweel, Ahmed A. Abdel-Rehim, "Energy and exergy analysis of a thermosiphon and forcedcirculation flat-plate solar collector using MWCNT/Water nanofluid", Case Studies in Thermal Engineering 14 (2019) 100416.

Nomenclature

$\sum \dot{m}_e$	Summation mass inlet to the control volume (kg/s)
$\sum \dot{m}_i$	Summation from the control volume (kg/s)
$\dot{Q}_{in}$	Rate of heat energy received bb the collector (kW)
$\dot{Q}_{out}$	Rate of heat loss (kW)
$\dot{Q}_{useful}$	Useful heat rate (kW)
$\dot{S}_g$	Entropy generation (kW)
$Ex_{c,p}$	Rate of exergy losses from FPSC surface to the absorber plate (kW)
$Ex_{dest.}$	Exergy destruction (kW)
$Ex_{f,i}$	Inlet exergy rate (kW)
$Ex_{f,o}$	Outlet exergy rate (kW)
$Ex_{p,e}$	Exergy losses from absorber plate to environmental (kW)
$Ex_{p,f}$	Rate of exergy losses between absorber plate and fluid (kW)
$Ex_{p,s}$	Exergy losses between absorber plate and the sun (kW)
$Ex_{sol.}$	Solar radiation exergy (kW)
Ex_{useful}	Exergy useful (kW)
F_R	Collector heat removal factor (-)
U_L	Overall heat transfer coefficient of the collector (kW/m^{2}K)
$\frac{d\Phi_{CV}}{dt}$	Rate of exergy change in control volume (kJ/kgK)
$\frac{dE_{CV}}{dt}$	Rate of energy change in control volume (kJ/kg)
$\frac{dS_{CV}}{dt}$	Rate of entropy change in control volume (kJ/kgK)
$\frac{dm_{CV}}{dt}$	Rate of mass change in control volume (kg/s)
h	Enthalpy (kJ/kg)

T	Temperature (K)
g	Gravity acceleration (m/s^2)
s	Entropy (kJ/kgK)
v	Velocity (m/s)
z	Elevation (m)
A	Area of the collector (m$^{2)}$
ASHRE	American Society of Heating, Refrigerating, and Air Conditioning Engineers
EES	Engineering equation solver
FPSC	Flat Plate Solar Collector
G	solar incident radiation fall on the earth (W/m^2)
Greek letters	
$(\tau\alpha)_\theta$	Transmittance τ of cover times absorptance α of plate at prevailing incident angle θ (-)
η_{ex}	Exergy efficiency (%)
η	Efficiency (%)
ψ	Exergy of flow (kW)
Subscripts	
a	Ambient
c	Collector
CV	Control volume
e	Outlet
f	Fluid
o	Reference condition
p	Plate
s	Sun